Jaroslav Vaculik and Michael C. Griffith

Probabilistic analysis of unreinforced brick masonry walls subjected to horizontal bending

Journal of Engineering Mechanics, 2017; 143(8):04017056-1-04017056-12

Published at: http://dx.doi.org/10.1061/(ASCE)EM.1943-7889.0001266

This is a pre-copyedited, author-produced version of an article accepted for publication in *ASCE Journal of Engineering Mechanics* following peer review. Publisher's version is available online at the following link:
doi: 10.1061/(ASCE)EM.1943-7889.0001266
Please cite as: Vaculik, J., and Griffith, M. C. (2017). "Probabilistic analysis of unreinforced brick masonry walls subjected to horizontal bending." *J Eng Mech*, 143(8).

Probabilistic Analysis of Unreinforced Brick Masonry Walls Subjected to Horizontal Bending

Jaroslav Vaculik[1]
and Michael C. Griffith[2]

ABSTRACT

Unreinforced masonry walls subjected to out-of-plane horizontal bending can fail by two alternate modes: stepped failure along the brick-mortar bond, or line failure cutting directly through the bricks. Because of random variations in material properties throughout a panel and the tendency for failure to occur across the weaker elements, vertical cracks will generally exhibit a combination of the two modes. This paper develops a pair of analytical methodologies which treat this phenomenon using a stochastic approach. The first part deals with calculating the ultimate moment capacity by allowing for the weakening effect associated with the mixed (stepped and line) mode of failure. This effect is quantified in terms of strength reduction factors for mean and characteristic (0.05 quantile) values of strength, which may be applied toward generic ultimate strength design. The second part deals with estimating the relative probability of each failure mode and the probability distribution for the relative proportions of each failure mode along a crack. This is of particular relevance to seismic performance, as the two failure modes lead to significantly different post-cracking behaviour.

Keywords: unreinforced masonry; walls; horizontal bending; out-of-plane; probabilistic; weak link

INTRODUCTION

The mechanical material properties of unreinforced masonry (URM) exhibit a high degree of variability compared to other structural materials such as steel or concrete. Sources of this variability include variations in the manufacturing process, quality of on-site workmanship, environmental conditions during manufacture and construction, as well as random variations in the materials themselves (Lawrence and Lu 1991). Nonetheless, probabilistic and reliability-based limit states design procedures for URM structures are considered less advanced than for other materials (Stewart and Lawrence 2002; Schueremans and Gemert 2006).

The flexural tensile bond strength of masonry (f_{mt}) is a key determinant of the ultimate out-of-plane load-carrying capacity of URM wall panels, and the fact that its variability has a significant influence on wall strength has long been recognised (Baker and Franken 1976). In conventional ultimate limit state design procedures for URM walls in bending, direct uncertainties arising from variability in the material strength properties are addressed by using their characteristic (lower 5th percentile) values, which is further followed by application of a strength reduction factor (inverse of a partial safety factor) to account for other uncertainties in the strength computation procedure. For example, the Australian Masonry Standard AS 3700 (Standards Australia 2011) prescribes a strength reduction factor of 0.6 for ultimate strength

[1]Postdoctoral Research Fellow, School of Civil, Environmental and Mining Engineering, The University of Adelaide, SA 5005, Australia; E-mail: jaroslav.vaculik@adelaide.edu.au (Corresponding author)

[2]Professor, School of Civil, Environmental and Mining Engineering, The University of Adelaide, SA 5005, Australia; E-mail: michael.griffith@adelaide.edu.au

design of walls in bending. However, the origin of such factors in masonry design codes can often be traced back to conversion from working stress design to equivalent limit state design rather than any rigorous reliability-based code-calibration, which means that the resulting safety levels are not precisely known (Stewart and Lawrence 2002). In order to overcome this and validate whether such factors are appropriate for design requires the development of procedures for estimating the probability of failure using a rational theoretical framework which incorporates the fundamental mechanics of out-of-plane URM wall response.

Over the years, numerous analytical studies have been undertaken to gain insight into the influence of random variability in mechanical properties on the out-of-plane behaviour of wall panels. The majority of these studies have tackled the problem through Monte Carlo simulation in which material properties are randomly assigned throughout the panel and the overall wall strength is then computed using a structural mechanics model. Early such works used elastic plate solutions and elastic finite element modelling (FEM) to quantify initial cracking loads of two-way spanning walls (Lawrence and Cao 1988; Lu and Lawrence 1991) as well as the ultimate (peak) strength in both vertically and horizontally spanning one-way walls (Lawrence 1991). In later work, Stewart and Lawrence (2002) described a generalised conceptual framework for studying the stochastic reliability of URM walls in flexure and also compared several alternate hypotheses in relation to load sharing between individual elements and their contribution to the overall panel strength. With ongoing advances in computational efficiency and modelling techniques for URM, recent works have employed nonlinear FEM to study the effects of material variability on the ultimate strength of vertically, horizontally and two-way spanning walls (Li et al. 2014; Li et al. 2016b; Li et al. 2016a). The outcomes of these studies have demonstrated favourable comparisons to experimental behaviour both in terms of wall capacities and failure mechanisms; however, due to the large computational effort and user expertise required to run such analyses, they are unsuitable for common use by designers. This creates the need for simplified 'design' techniques for estimating wall strength, which recognise the fundamental mechanics involved in out-of-plane flexural response whilst adequately accounting for the stochastic influence of the material properties.

The present paper will focus on development of such methodology for brick URM walls subjected to horizontal bending. Pure horizontal bending corresponds to an out-of-plane flexural moment whose axis is oriented vertically, and can be generated by applying a lateral load to a wall supported along its vertical edges using the arrangement shown in Figure 1. In full masonry panels within overall buildings, boundary conditions to generate pure horizontal bending are not very common; however, the internal stress condition is approached in common two-way spanning wall arrangements such as those shown in Figure 2 where horizontal bending causes the formation of vertical crack lines in localised regions.

This paper will consider specifically single-leaf brickwork utilising a regular stretcher bond pattern (refer Figure 1). In this type of masonry, vertical cracks can form by two distinct modes [Figure 3 (a) and (b)]: *stepped failure* where the crack follows a toothed pattern along the brick-mortar bond of bed joints and perpend joints, or *line failure* where the crack cuts across brick units and perpend joints in a straight line. The tendency for either mode to be favoured depends on the relative material strengths of the brick units and the masonry bond. Vertical cracks rarely exhibit either of these failure modes exclusively; instead they tend to develop a combination of the two as a result of local variation in the material properties throughout the panel (Figure 3c). This has been experimentally demonstrated through tests on both small-sized specimens and full-scale walls (Lawrence 1995; Willis et al. 2004; Griffith et al. 2007; Griffith and Vaculik 2007). And although advances have been made in development of simple mechanics-based expressions for calculating the ultimate moment capacity with respect to each failure mode for the purpose of design (Willis et al. 2004), these methods ignore the fact that these modes can occur simultaneously. This gives rise to several issues which will now be described in the context of the aims of this paper.

Firstly, the conventional approach for calculating the design strength of URM in horizontal bending involves separately calculating the moment capacities for the stepped and line failure

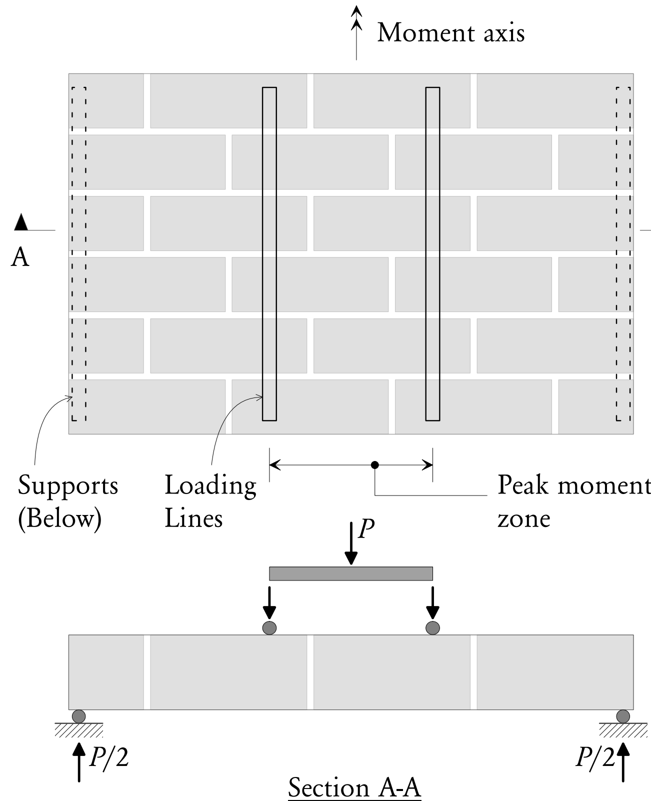

FIG. 1: Typical wallette beam test setup in which the specimen is subjected to pure horizontal bending [identical to arrangement used by Willis et al. (2004)]. The brick masonry shown is built with half-overlap stretcher bond.

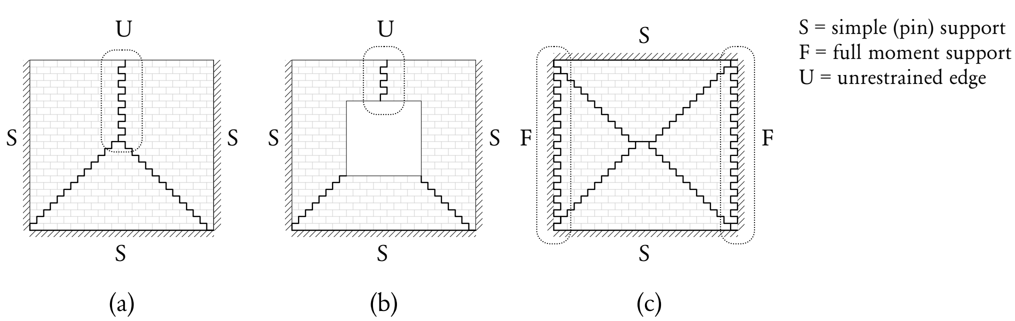

FIG. 2: Examples of horizontal bending regions in two-way spanning walls shown using idealised cracking patterns. Horizontal bending regions are characterised by formation of vertical cracks (highlighted). For clarity, all vertical cracks are shown as stepped.

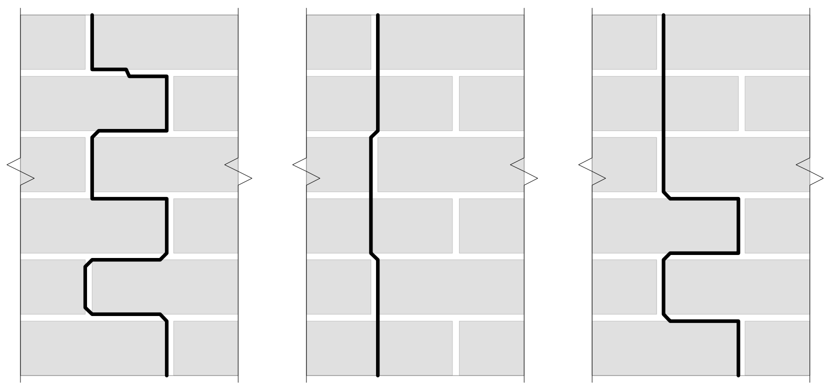

(a) Pure stepped failure (b) Pure line failure (c) Typical example of mixed failure

FIG. 3: Different possible failure modes in horizontal bending: (a) Pure stepped failure; (b) Pure line failure; (c) Typical example of mixed failure.

modes using characteristic values of material properties and adopting the lower value (e.g. AS 3700). However, because crack formation is governed by weak link effects, it can be easily shown that the characteristic strength of the mixed (stepped and line) failure mode will always be lower than for either mode considered separately [e.g. using equation (21) provided later in this paper]. Thus by ignoring these stochastic effects, the conventional design approach has the potential to be unconservative. The first analytical method proposed in this paper deals with quantifying the weakening influence on the ultimate strength arising from weak link effects. Unlike most previous analytical research into the influence of stochastic effects on URM bending strength which has utilised Monte Carlo simulation, the present paper tackles the problem through formulation of mechanics-based governing equations suitable toward design. It is the intent that these equations can be subsequently incorporated into a generalised virtual work approach (e.g. Lawrence and Marshall 2000; Baker et al. 2005; Vaculik et al. 2014), analogous to yield line analysis, in order to predict the ultimate out-of-plane strength of two-way spanning walls.

Secondly, the mode of failure generated at the cracking stage has a major effect on the residual (post-cracking) behaviour of the crack which influences the wall's out-of-plane seismic performance. This follows from the fact that interlocking units along a stepped crack are able to maintain some residual strength via frictional mechanics and also contribute toward hysteretic damping under cyclic loading (Griffith et al. 2007). By contrast, line failure is brittle and has no residual moment capacity. A further detrimental effect can occur in two-way spanning walls (e.g. Figure 2c) where excessive line cracking along the supported vertical edges can cause the mechanism to revert from two-way bending to one-way vertical bending, as observed in tests by Griffith et al. (2007). Such effects are particularly important in URM structures, where alternate modes of brittle failure caused by variation of material properties and wall configurations can lead to significantly different post-cracking behaviour and therefore affect seismic performance (e.g. Foraboschi and Vanin 2013). The contrasting post-cracking behaviour of stepped and line cracks highlights the need to develop an analytical technique for predicting their relative proportions along a crack, which is undertaken in the second half of this paper. It is anticipated that the developed methodology could be incorporated as part of a limit analysis out-of-plane wall assessment procedure that ignores the bond strength (e.g. Orduña and Lourenço 2005; Foraboschi 2014; Vaculik et al. 2014; Lagomarsino 2015; Casapulla and Portioli 2015).

THEORETICAL MODEL

The basis of the model is to formulate the probability distributions of the individual (stepped

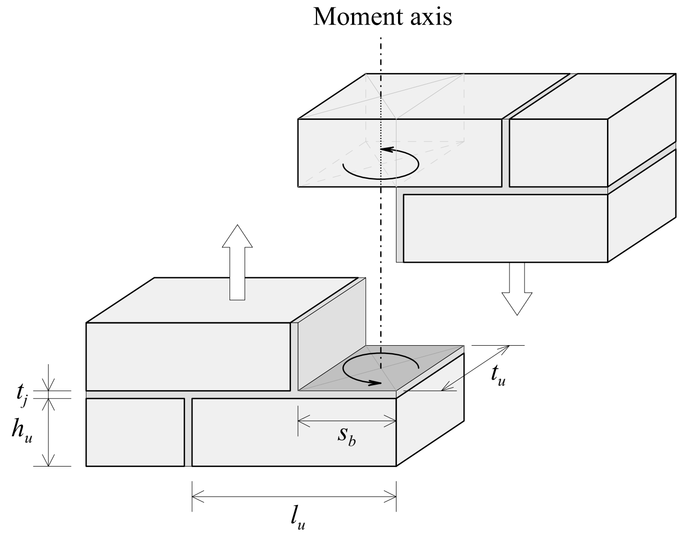

FIG. 4: Torsion about the centroid of a bed joint.

and line) failure modes by treating the key material properties as random variables. Then by applying the weak link concept, the strength distribution of the mixed mode of failure as well as the relative likelihood of either failure mode can be determined.

Moment Capacities for Basic Failure Modes

The upcoming analytical expressions are applicable specifically to single-leaf stretcher bond masonry which is illustrated in Figure 4. Although alternate masonry bond patterns could also be considered within the generalised stochastic framework proposed in this paper, refinement of the fundamental moment capacity expressions would be necessary to suit such patterns.

Stepped Failure: Over a single masonry course, the ultimate moment capacity with respect to stepped failure (Figure 3a) is calculated as

$$m_{u\,\mathrm{step}} = k_{be}\,\tau_{um}\,t_u^3, \tag{1}$$

which represents the torsional strength of a rectangular bed joint with thickness t_u and overlap s_b (Figure 4). In half overlap stretcher bond masonry, s_b is calculated as

$$s_b = (l_u - tj)\,/2, \tag{2}$$

where l_u is the length of the brick unit, and t_j is the mortar joint thickness. The expression assumes that the joint fails once the maximum shear stress along the section as determined by elastic theory (Timoshenko and Goodier 1934) reaches the shear stress capacity of the bond, τ_{um}. Due to the well-established experimental observation that perpend joints crack early in the response (Base and Baker 1973; Lawrence 1995) any flexural contribution from perpend joints is omitted. Parameter k_{be} is a dimensionless coefficient relating the maximum shear stress in a rectangular section to the applied torsion and is equal to 0.208 for square overlap ($s_b = t_u$). Equation (1) incorporates a slight refinement to an expression originally proposed by Willis et al. (2004) in order to make it applicable to any overlap aspect ratio (s_b/t_u) as controlled through k_{be}. Values of k_{be} for bond patterns with generic values of overlap are provided in Vaculik (2012).

To estimate τ_{um} within equation (1), Willis et al. (2004) proposed the expression

$$\tau_{um} = r f_{mt} + \mu\sigma_v, \tag{3}$$

where f_{mt} is the flexural tensile strength of the masonry and σ_v is the vertical stress acting normal to the bed joint, whose respective coefficients were empirically calibrated as $r = 1.6$ and $\mu = 0.9$ using small brickwork wallette tests.

It is worth noting that equations (1) and (3) represent uniaxial horizontal bending and ignore any vertical bending on the section (i.e. biaxial bending) which would generate an eccentricity of the acting normal stress. This is due to several reasons: The main practical application of these moment capacity expressions is within a virtual work approach for estimating the strength of two-way walls (Figure 2), and in such methods the actual internal moment demands along cracks are not explicitly calculated, nor is it easy to calculate them. Additionally, in zones where vertical cracks are generated, internal moment from vertical bending is generally expected to be small in comparison to horizontal bending. Furthermore, the influence of a non-uniform vertical stress distribution on the bed joint torsional capacity is expected to be relatively minor in mortared masonry [due to dominance of the cohesion term in equation (3)] in comparison to dry-joint masonry where friction provides the entirety of the resistance and therefore such effects become much more important (Casapulla and Portioli 2015).

Line Failure: Over a single course, the moment capacity with respect to line failure is calculated using the following expression by Willis et al. (2004):

$$m_{u\,\mathrm{line}} = \frac{1}{2}\,(f_{ut} - \nu_u\,\sigma_v)\,\frac{h_u t_u^2}{6}, \tag{4}$$

where f_{ut} is the lateral modulus of rupture of the brick unit, ν_u is the Poisson's ratio of the brick units (typically taken as 0.2), h_u is the height of the brick unit, and other variables as defined previously. The capacity given by equation (4) is based entirely on the tensile strength of the brick unit, and similarly to equation (1) it ignores any contribution from the perpend joint. The expression also allows for the weakening influence on the flexural strength of the unit arising from vertical axial load and Poisson's effect.

The accuracy of equations (1)–(4) was originally validated by Willis et al. (2004) using flexural tests on brick masonry wallettes (equivalent to that shown in Figure 1) by counting the number of failed bed joints and bricks in each test specimen and summing their moment contributions toward the overall crack. These calculations produced favourable correlation with measured moment capacities; however, this validation process required a posteriori knowledge of the relative proportions of each failure mode. Nonetheless, the fact that the expressions were validated this way provides a sound basis for the development of the analysis techniques proposed in this paper which are applicable a priori.

General Assumptions

The following general assumptions are made:

1. Local crack formation is assumed to be governed by the weak link concept applied over a single course of bricks. A basic module over two courses is illustrated in Figure 5, where it is seen that stepped failure occurs when two bed joints fail in torsion, or line failure occurs when a single brick fails in flexure. The moment capacity of the mixed failure mode over a single course is taken as the lesser of equations (1) and (4), that is:

$$m_{u\,\mathrm{mix}} = \min(m_{u\,\mathrm{step}}, m_{u\,\mathrm{line}})\,. \tag{5}$$

2. Material properties f_{mt} and f_{ut} are treated as randomly distributed variables. It is assumed that these can be adequately represented by any of the normal, lognormal and Weibull distributions, as substantiated in various works (Baker and Franken 1976; Lawrence 1985; Heffler et al. 2008; Vaculik 2012). The typical range of variability of these properties expressed as the coefficient of variation (CoV) (standard deviation divided by

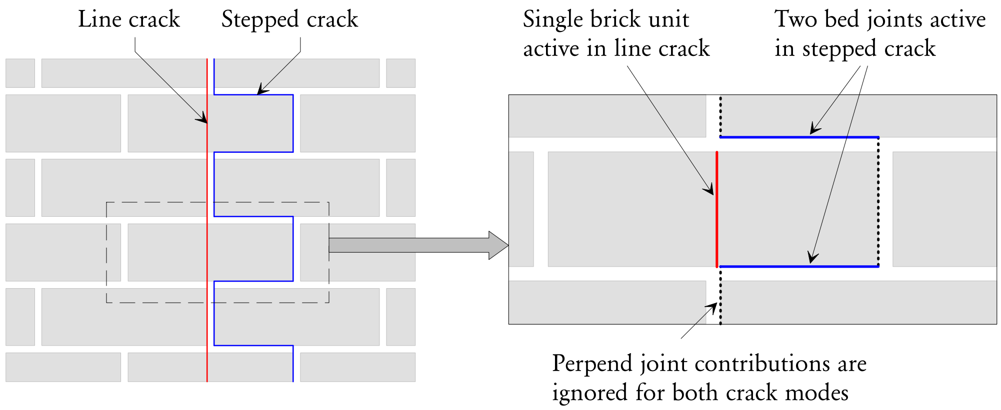

FIG. 5: Basic masonry module consisting of two courses of bricks.

the mean) is between 0.15 and 0.5, as demonstrated in the aforementioned references as well as in-situ testing (McNeilly et al. 1996).

3. All other parameters in the governing equations (1)–(4) including brick unit and mortar joint dimensions, axial stress, and Poisson's ratio are treated as constants.

ULTIMATE STRENGTH CAPACITY

This section describes the procedure for computing the ultimate strength of the mixed failure mode allowing for the weak link effect. Further to the assumptions stated previously, it will be assumed that the peak moment capacities of the stepped and line failure modes are reached simultaneously. This allows the total moment capacity to be taken as the direct sum of the individual mode contributions. As mentioned previously, work by Willis et al. (2004) demonstrated that calculations made on this basis produced good correlation with experimental results. Because the characteristic strength is of particular interest towards design, f_{mt} and f_{ut} will be represented using either of the lognormal and Weibull two-parameter distributions which adopt only positive values and thus provide more representative behaviour at the lower end tail (compared to the normal distribution).

Non-dimensional formulation of the governing equations

For convenience, let us consider the strength in horizontal bending in terms of the non-dimensionalised *orthogonal strength ratio*, η, as this convention is often adopted in the literature (e.g. Sinha 1978; Seward 1982) including Eurocode 6 (Comité Européen de Normalisation 2005):

$$\eta = \bar{M}_h / \bar{M}_v, \tag{6}$$

where $\bar{M}_h$ and $\bar{M}_v$ are the moment capacities for horizontal and vertical bending, respectively, in terms of the moment per unit length of the crack [N.B. The definition of the orthogonal strength ratio in the literature is sometimes interchanged between equation (6) and its inverse].

It is also useful to define the non-dimensional quantities

$$F_{ut} \equiv \widehat{f}_{ut} / \widehat{f}_{mt}, \tag{7}$$

and

$$\Sigma_v \equiv \sigma_v / \widehat{f}_{mt}, \tag{8}$$

where $\widehat{f}_{mt}$ and $\widehat{f}_{ut}$ are mean values of the respective properties.

Recognising that in the absence of vertical compressive stress, the mean vertical bending moment capacity per unit length of crack is

$$\bar{M}_v = \widehat{f}_{mt} \frac{t_u^2}{6}, \tag{9}$$

and converting the moment over a single course (m) to a moment per unit length ($\bar{M}_h$) using $\bar{M}_h = m/(h_u + t_j)$, the orthogonal strength ratios for stepped failure and line failure are obtained by substituting equations (1), (3), (4), (8), and (9) into (6), which gives

$$\eta_{\text{step}} = \underbrace{k_{\text{step}}\, r\, \frac{f_{mt}}{\widehat{f}_{mt}}}_{=\eta_{\text{step,rand}}} + \underbrace{k_{\text{step}}\, \mu\, \Sigma_v}_{=\eta_{\text{step,const}}}, \tag{10}$$

and

$$\eta_{\text{line}} = \underbrace{k_{\text{line}}\, \frac{f_{ut}}{\widehat{f}_{mt}}}_{=\eta_{\text{line,rand}}} \underbrace{- k_{\text{line}}\, \nu_u\, \Sigma_v}_{=\eta_{\text{line,const}}}. \tag{11}$$

All information in equations (10) and (11) that relates to unit geometry is contained within the constants

$$k_{\text{step}} = \frac{6\, k_{be}\, t_u}{h_u + t_j}, \tag{12}$$

and

$$k_{\text{line}} = \frac{h_u}{2\,(h_u + t_j)}. \tag{13}$$

PDFs and CDFs

The moment capacities of the individual failure modes [equations (10) and (11)] each contain a random component proportional to the material strength (f_{mt} or f_{ut}), plus a constant component due to vertical stress. Each random component must have the same type of underlying distribution and CoV as the related material property. For a generic parameter X, let us use $\mathbb{E}\langle X\rangle$ to denote its expected value (mean), and $\mathbb{C}\langle X\rangle$ to denote its CoV. The random component of capacity in stepped failure, $\eta_{\text{step,rand}}$, is distributed such that:

$$\mathbb{E}\langle \eta_{\text{step,rand}}\rangle = k_{\text{step}}\, r, \tag{14}$$

$$\mathbb{C}\langle \eta_{\text{step,rand}}\rangle = \mathbb{C}\langle f_{mt}\rangle\,. \tag{15}$$

Similarly, for line failure:

$$\mathbb{E}\langle \eta_{\text{line,rand}}\rangle = k_{\text{line}}\, F_{ut}, \tag{16}$$

$$\mathbb{C}\langle \eta_{\text{line,rand}}\rangle = \mathbb{C}\langle f_{ut}\rangle\,. \tag{17}$$

From this, the probability density functions (PDFs) and cumulative distribution functions (CDFs) of η_{step} and η_{line} can be formulated. For stepped failure, the PDF at the value $\eta = x$ is

$$p_{\eta_{\text{step}}}(x) = p_{\eta_{\text{step,rand}}}(x - \eta_{\text{step,const}})\,, \tag{18}$$

and the CDF is

$$P_{\eta_{\text{step}}}(x) = P_{\eta_{\text{step,rand}}}(x - \eta_{\text{step,const}})\,. \tag{19}$$

The same can be rewritten for line failure.

Since the weak link hypothesis [equation (5)] defines η_{mix} as the lesser of pairs of random variables drawn from η_{step} and η_{line}, according to joint probability theory the PDF and CDF of the mixed failure mode are, respectively

$$p_{\eta_{\text{mix}}}(x) = p_{\eta_{\text{step}}}(x)\,[1 - P_{\eta_{\text{line}}}(x)] + p_{\eta_{\text{line}}}(x)\,\left[1 - P_{\eta_{\text{step}}}(x)\right], \tag{20}$$

and

$$P_{\eta_{\text{mix}}}(x) = P_{\eta_{\text{step}}}(x) + P_{\eta_{\text{line}}}(x) - P_{\eta_{\text{step}}}(x)\, P_{\eta_{\text{line}}}(x)\,. \tag{21}$$

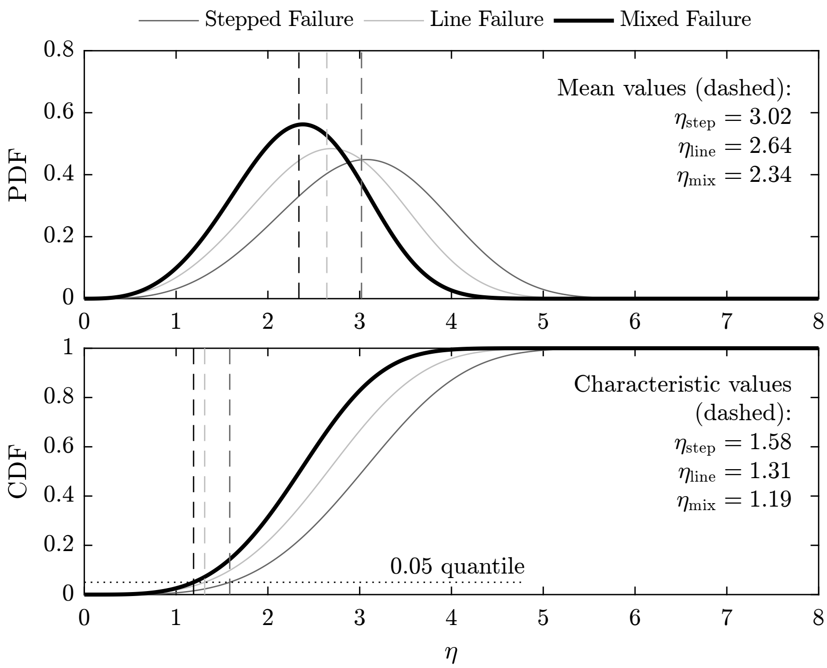

FIG. 6: Example of predicted probability distribution functions (PDF top, CDF bottom) for the strength (η) of the stepped, line and mixed failure modes. The example considers $230 \times 110 \times 76$ mm units and 10 mm thick mortar joints, with $F_{ut} = 6$ and $\Sigma_v = 0.1$. Material properties f_{mt} and f_{ut} are modelled by Weibull distribution with CoV = 0.3. The functions demonstrate that the strength of the mixed failure mode is lesser than either of the fundamental modes considered individually.

The model described is suited for implementation using computer software where the PDFs and CDFs of the probability distributions of interest can be programmed-in as functions. Figure 6 portrays an example which considers standard Australian clay brick units with dimensions $230 \times 110 \times 76$ mm ($l_u \times t_u \times h_u$) and 10 mm thick mortar joints (t_j), and furthermore assumes that $\nu_u = 0.2$, $r = 1.6$ and $\mu = 0.9$ (Willis et al. 2004). In this example, the ratio of brick strength to bond strength is $F_{ut} = 6$ and the ratio of axial stress to bond strength is $\Sigma_v = 0.1$. The Weibull distribution is used to represent f_{mt} and f_{ut} at CoV = 0.3. The plots demonstrate the reduction in strength caused by weak link effects for both mean and characteristic values.

Mean and characteristic values of strength

The mean values of η_{step} and η_{line} can be obtained directly by assigning mean values of the respective tensile strengths f_{mt} and f_{ut} into equations (10) and (11), which gives

$$\mathbb{E}\langle \eta_{\text{step}} \rangle = k_{\text{step}} \left(r + \mu \, \Sigma_v \right) , \tag{22}$$

and

$$\mathbb{E}\langle \eta_{\text{line}} \rangle = k_{\text{line}} \left(F_{ut} - \nu_u \, \Sigma_v \right) . \tag{23}$$

The mean value of η_{mix} however has to be computed numerically, since its PDF and CDF as given by equations (20) and (21) will not generally follow any common distribution. This can be done by numerically integrating the first moment of the PDF.

Characteristic values of η_{step}, η_{line} and η_{mix} are also easily obtained numerically by solving for the η value at which the CDF equals 0.05.

Strength reduction factors

A convenient way to quantify the weakening effect is in terms of a strength reduction factor (ϕ), defined as the ratio of the strength of the mixed failure mode to the lesser of strengths for the individual modes; i.e. for mean strength:

$$\phi_{\text{mean}} = \frac{\mathbb{E}\langle \eta_{\text{mix}} \rangle}{\min(\mathbb{E}\langle \eta_{\text{step}} \rangle, \mathbb{E}\langle \eta_{\text{line}} \rangle)}. \tag{24}$$

and for characteristic strength:

$$\phi_{\text{char}} = \frac{\text{Char}\langle \eta_{\text{mix}} \rangle}{\min(\text{Char}\langle \eta_{\text{step}} \rangle, \text{Char}\langle \eta_{\text{line}} \rangle)}, \tag{25}$$

For example, in the scenario shown in Figure 6, the mean-strength reduction factor is $\phi_{\text{mean}} = 2.34/2.64 = 0.89$, and the characteristic-strength reduction factor is $\phi_{\text{char}} = 1.19/1.31 = 0.91$. Therefore in limit state design, which uses characteristic properties, weak link effects would generate a 9% reduction in strength compared to the conventionally calculated value, e.g. according to AS 3700 (Standards Australia 2011).

To examine conditions under which the strength reduction becomes most severe, ϕ_{mean} and ϕ_{char} were computed for standard Australian clay brick masonry in terms of F_{ut} versus Σ_v as plotted in Figure 7. Material strengths f_{mt} and f_{ut} were represented using the Weibull distribution, and their CoV of was taken as 0.3 which is considered typical.

A notable feature of Figure 7 is the presence of distinct regions in the F_{ut}-Σ_v space where the reduction in strength is most pronounced. These occur where the strengths of the individual failure modes are similar in magnitude, thus causing the mixed failure mode to become dominant. The graphs also demonstrate that the most adverse strength reduction occurs at zero axial stress ($\Sigma_v = 0$) at $F_{ut} \approx 6.5$. This critical value of F_{ut} can be calculated as

$$\text{critical } F_{ut} = r\,\frac{k_{\text{step}}}{k_{\text{line}}}. \tag{26}$$

It is worth noting that $F_{ut} = 6.5$ is well within the typical range observed in practice; hence, these effects should not be ignored.

The greatest possible strength reduction that can occur at a given level of material strength variability (as CoV) is plotted in Figure 8. It is seen that the reduction is sensitive to the type of distribution chosen to represent the material properties, and that the Weibull distribution is associated with a greater reduction in strength than the lognormal distribution. The difference between the two distributions is greatest in relation to the characteristic strength. This trend can be explained by the fact that the Weibull distribution has a fatter lower end tail than the lognormal distribution.

The plot in Figure 8 also demonstrates that considerable strength reduction can develop at typical levels of material strength variability. For instance, at CoV = 0.3, which is deemed typical on the basis of in-situ tests by McNeilly et al. (1996), there is a 17% reduction in strength. At CoV = 0.5, which is the largest level of variability observed in that study, a 28% reduction occurs. Nonetheless, allowance for this level of reduction appears to be adequately provided by the capacity reduction factor $\phi = 0.6$ prescribed by AS 3700 for bending design.

EXPECTED LIKELIHOOD OF EACH FAILURE MODE

For the purpose of estimating the relative probabilities of each failure mode, it will be assumed that f_{mt} and f_{ut} follow the normal distribution, which allows for some useful simplifications of the governing formulae. Allowance is also made to treat Poisson's ratio of the brick unit (ν_u) as a normally distributed random variable.

Probability of Each Failure Mode in a Single Course

Let us consider the probability of stepped failure, denoted as P_{step}, which occurs when $m_{u\,\text{step}} < m_{u\,\text{line}}$. Using equations (1)–(4) this can be written as

$$r f_{mt} + \mu\,\sigma_v < G_h\,(f_{ut} - \nu_u\,\sigma_v)\,, \tag{27}$$

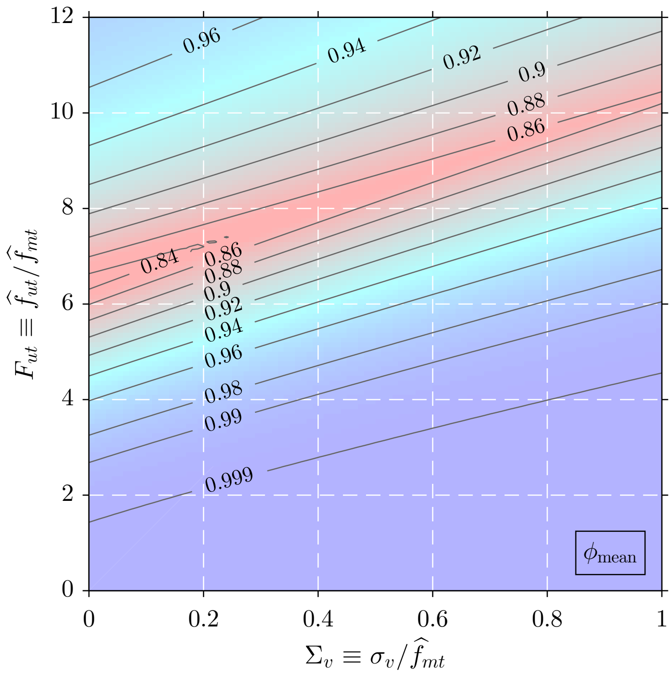

(a) Mean-strength reduction factor, ϕ_{mean}.

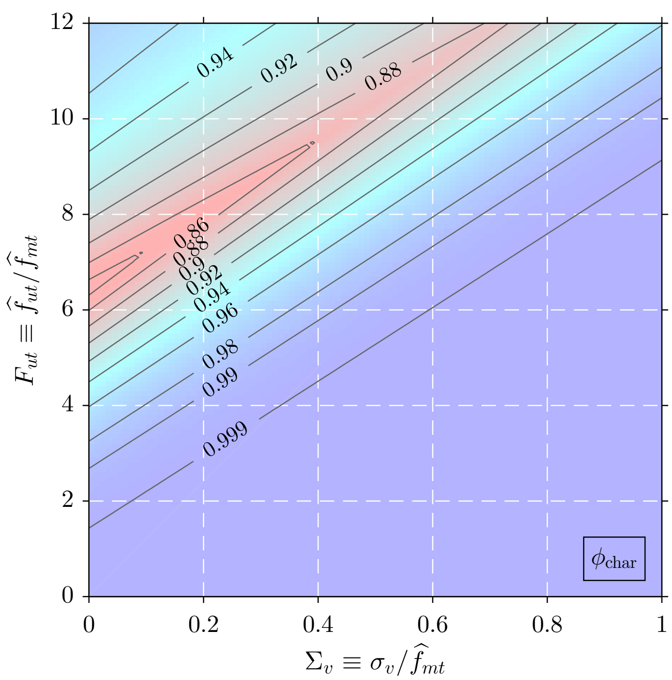

(b) Characteristic-strength reduction factor, ϕ_{char}.

FIG. 7: Isolines of strength reduction factors for clay brick masonry with $230 \times 110 \times 76$ mm units and 10 mm thick mortar joints. Material properties f_{mt} and f_{ut} are modelled by Weibull distribution with CoV $= 0.3$. The plots demonstrate distinct regions in the F_{ut}-Σ_v space where the weak link effect is most pronounced, which coincides with zones where the strength of the individual modes are comparable in magnitude.

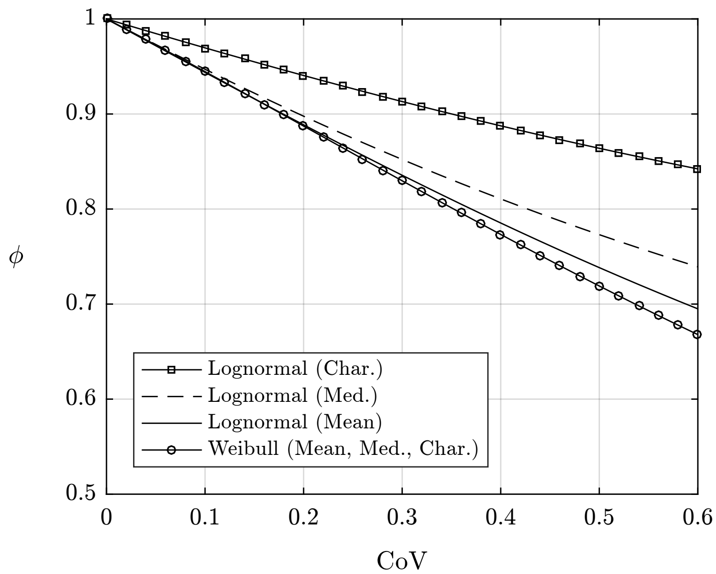

FIG. 8: Strength reduction factors corresponding to the maximum possible strength reduction that can occur at any given level of material strength (f_{mt} and f_{ut}) variability as defined by the CoV. This point of maximum strength reduction corresponds to the critical value of F_{ut} as given by equation (26).

where

$$G_h = \frac{k_{\text{line}}}{k_{\text{step}}} = \frac{h_u}{12\, t_u\, k_{be}}. \tag{28}$$

Inequality (27) contains the randomly distributed variables f_{mt}, f_{ut} and ν_u. By assuming that each is normally distributed, the inequality can be reduced to $0 < u$, where u is a normally distributed dummy variable which has the mean

$$\mathbb{E}\langle u\rangle = G_h F_{ut} - r - \Sigma_v \left(G_h \mathbb{E}\langle \nu_u\rangle + \mu\right), \tag{29}$$

and variance

$$\mathbb{S}\langle u\rangle^2 = \left(G_h F_{ut} \mathbb{C}\langle f_{ut}\rangle\right)^2 + \left(r \mathbb{C}\langle f_{mt}\rangle\right)^2 + \left(\Sigma_v G_h \mathbb{E}\langle \nu_u\rangle\, \mathbb{C}\langle \nu_u\rangle\right)^2. \tag{30}$$

From this, the basic probability that a single course undergoes stepped failure (P_{step}) is determined by computing the probability that $u > 0$, such that

$$P_{\text{step}} = 1 - P_{\text{line}} = \Pr(u > 0) = \Phi_N\left(\frac{\mathbb{S}\langle u\rangle}{\mathbb{E}\langle u\rangle}\right), \tag{31}$$

where $\Phi_N(\cdots)$ is the CDF of the standard normal distribution.

The solution of equation (31) is illustrated for standard Australian clay brick units and CoV $= 0.3$ in Figure 9, by plotting contour lines of the probability of stepped failure versus F_{ut} and Σ_v. The figure demonstrates that stepped failure becomes more likely as the brick-to-bond strength ratio (F_{ut}) increases, and less likely at higher levels of axial stress (Σ_v). This latter trend arises due to a combination of axial stress having both a strengthening influence on stepped failure due to internal friction and a weakening influence on line failure due to Poisson's effect.

The influence of higher variability (CoV) in the material properties (f_{mt}, f_{ut} and ν_u) on the plot in Figure 9 would be to increase the spread of the contour lines relative to the median

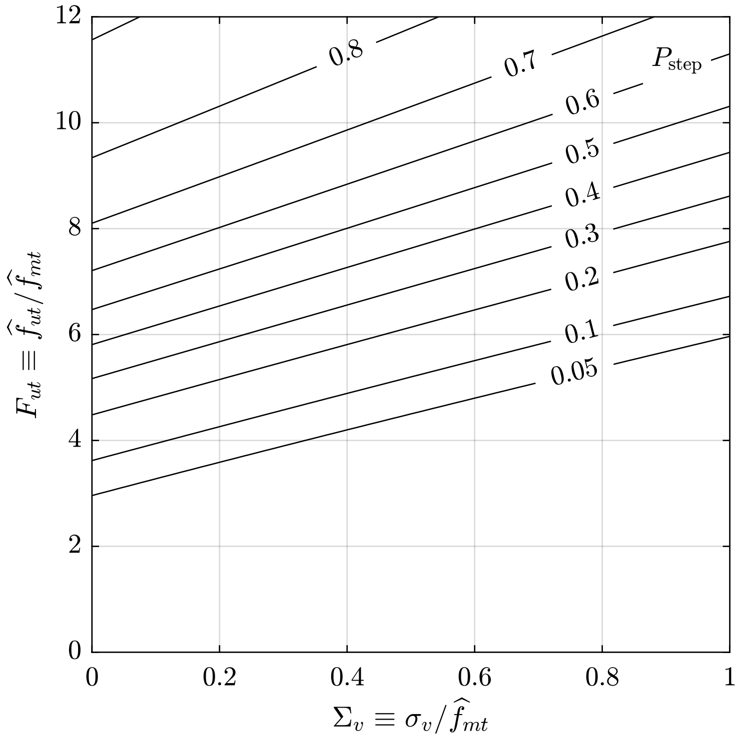

FIG. 9: Isolines of the probability of stepped failure ($P_{\text{step}} = 1 - P_{\text{line}}$) for clay brick masonry with $230 \times 110 \times 76$ mm units and 10 mm thick mortar joints. Material properties f_{mt} and f_{ut} are modelled by normal distribution with CoV $= 0.3$.

contour line, whereby the median contour line corresponds to $P_{\text{step}} = 0.5$ and represents equal probability of stepped and line failure. In other words, masonry with highly variable material properties will tend to develop closer amounts of stepped and line failure. The median contour line is unaffected by the CoV and can be determined from equation (29) by setting $\mathbb{E}\langle u \rangle = 0$.

Relative Proportions of Each Failure Mode

An example of a potential practical application of the developed methodology would be in predicting the residual moment capacity of a vertical crack, where it is necessary to be able to estimate the relative proportion of each failure mode. Let us denote the proportion of stepped failure as R_{step}, the total number of courses as n, and the number of courses undergoing stepped failure as k. If we assume that all masonry courses are independent in terms of their material properties, then k will follow the binomial distribution and have the CDF:

$$\Pr(X \leq k) = \sum_{i=0}^{k} \frac{n!}{i!(n-i)!} {P_{\text{step}}}^{i} \left(1 - P_{\text{step}}\right)^{n-i}, \tag{32}$$

from which the proportion of stepped failure is determined as $R_{\text{step}} = k/n$.

Over any number of courses (n), the expected value of R_{step} is equivalent to P_{step}. However, the characteristic (0.05 quantile) value of R_{step}, which may be of interest in design, becomes dependent on n as plotted in Figure 10. It is seen that $\text{Char}\langle R_{\text{step}} \rangle$ decreases with reducing n, and conversely, it asymptotically approaches P_{step} as n increases. This is because over a large number of courses it is less likely that R_{step} will deviate significantly from P_{step}, whereas over fewer courses it becomes more likely.

COMPARISON WITH EXPERIMENT

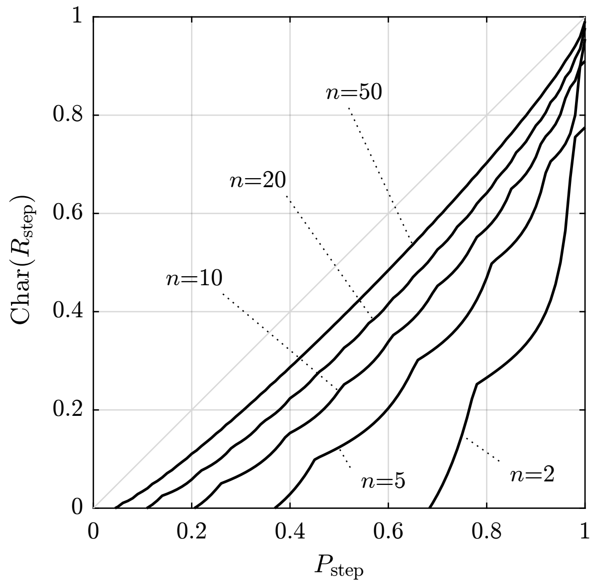

FIG. 10: Characteristic value of the proportion of stepped failure (R_{step}) versus the basic probability of stepped failure (P_{step}) for varying number of masonry courses. Over a large number of courses $\mathrm{Char}\langle R_{\mathrm{step}}\rangle$ approaches P_{step}, but if the number of courses is small then $\mathrm{Char}\langle R_{\mathrm{step}}\rangle$ can become considerably smaller than P_{step}.

Tests on Small-Sized Wallettes

Accuracy of the analytical methods was examined using results of bending tests on small-sized wallettes undertaken by Willis (2004) (also reported in Willis et al. 2004). It is important to note that these tests were part of the data set that Willis used to calibrate the empirical parameters r and μ in equation (3), and as such, one would expect the correlation between the measured and predicted moment capacity to already be good. However, since the main focus of the present comparisons is the stochastic nature of response, which was not previously addressed by Willis, the use of this data set is still valuable.

This experimental study involved four-point-bending tests on wallettes 6 courses tall and 3.5 bricks long (approx. 440 mm by 840 mm) using the arrangement shown in Figure 1. The wallettes were constructed using $230 \times 114 \times 65$ mm clay brick units and 10 mm mortar joints. It is worth noting that the constant peak moment zone was applied across a length of a single half-overlap bed joint (s_b as shown in Figure 4) to facilitate failure within this zone. Five sets of tests were performed: In the first four, the walls were oriented vertically and subjected to different levels of precompression levels, including 0, 0.075, 0.15, and 0.25 MPa. The fifth set involved walls oriented horizontally with no precompression. Each set included five repetitions, giving a total of 25 individual tests. Material properties f_{mt} and f_{ut} were quantified separately through material tests on the individual batches of mortar and brick units used in the construction of the wallettes—f_{mt} was quantified using bond the wrench test as prescribed by AS 3700, and f_{ut} was determined from four-point-bending tests on beam specimens comprising three bricks glued together end-to-end. From these tests, mean values and CoVs of the properties were quantified for use in the present analysis (Table 1).

Figure 11 compares the measured strength to predictions made using two alternate approaches: firstly with the 'conventional' approach as the direct minimum of the mean values for stepped and line failure (Figure 11a), and secondly with the developed stochastic approach where the mean strength was computed as the first moment of the PDF defined by equation (20) (Figure 11b). Additional detail of these analyses is presented in Table 1, including material

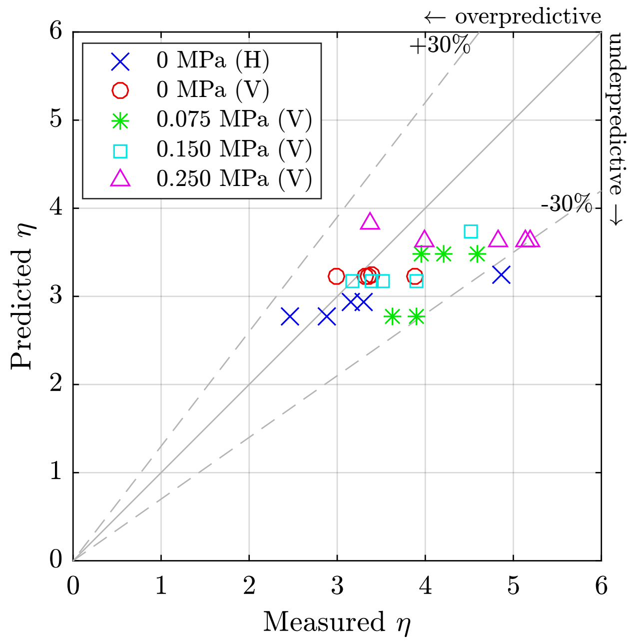

(a) Strength calculated as minimum of stepped and line failure (conventional approach).

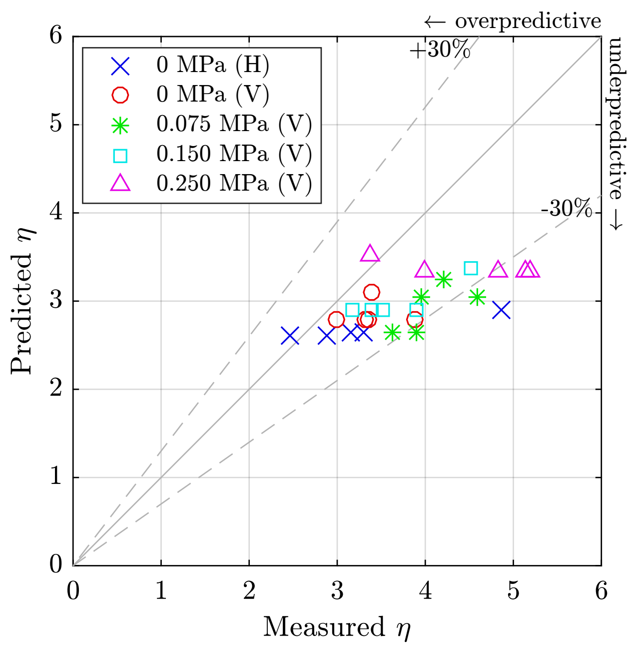

(b) Strength calculated using the mixed failure mode (proposed approach).

FIG. 11: Comparison of predicted and experimentally measured ultimate strength in small-sized (six course) wallettes. Predicted values were calculated using mean values and CoVs of material properties measured experimentally.

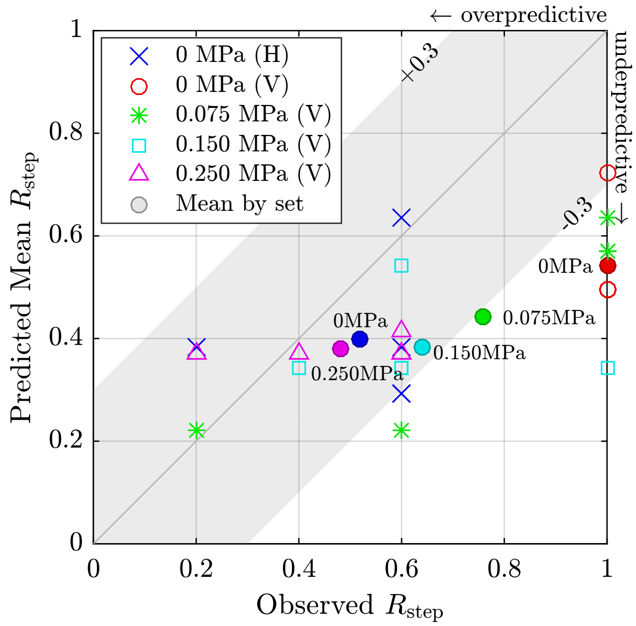

FIG. 12: Comparison of predicted and experimentally observed proportion of stepped failure in small-sized (six course) wallettes. Mean values for each precompression data set are shown using solid circles. Predicted values were calculated using mean values and CoVs of material properties measured experimentally.

properties, analysis results, and experimental results for each specimen. The average ratio of the predicted to experimental strength is 0.88 for the conventional method and 0.80 for the stochastic method. That the conventional method gives slightly closer correlation with the test results is not surprising given that this data set was used by Willis to calibrate the coefficients in equation (3). It is also possible that by not allowing for the stochastic effects, these coefficients may have been slightly underestimated in Willis' calibration process.

For the same data set, the proportion of stepped failure observed experimentally is compared to the value predicted using equation (31) in Figure 12. The plot demonstrates fairly large scatter in the individual experimental values of R_{step}, which is not unexpected given the small number of courses in each wallette ($n = 5$). By considering the mean values at each level of precompression (solid circles in Figure 12), it can be seen that both the experimental and predicted values exhibit a trend where R_{step} reduces with increasing precompression (with the exception of the 'H' specimens). On average, the proposed method underpredicts R_{step} in the test specimens by a difference of 0.25 indicating that it is slightly conservative.

The fact that the proposed methodology underestimates the strength of the wallettes (Figure 11b) while underpredicting the proportion of stepped failure (Figure 12) suggests that Willis' expression [equation (4)] may be slightly underestimating the basic strength in line failure, possibly because it ignores any flexural contribution from the perpend joints. It is worth noting that the line failure moment capacity expression presently prescribed in AS 3700 includes both a brick flexure component (f_{ut}-proportional) plus a perpend flexure component equal to the full elastic moment capacity of the perpend section ($f_{mt}\,Z$); however as evidenced experimentally, a full contribution from perpends is not justifiable due to early cracking (Base and Baker 1973; Lawrence 1995). It is nonetheless conceivable that a partial contribution from perpends may still be active at the point that the brick units reach their peak flexural strength, which is supported by the present results. Modification of the proposed stochastic methodology to include a f_{mt}-proportional perpend contribution into equation (4) would be relatively straightforward.

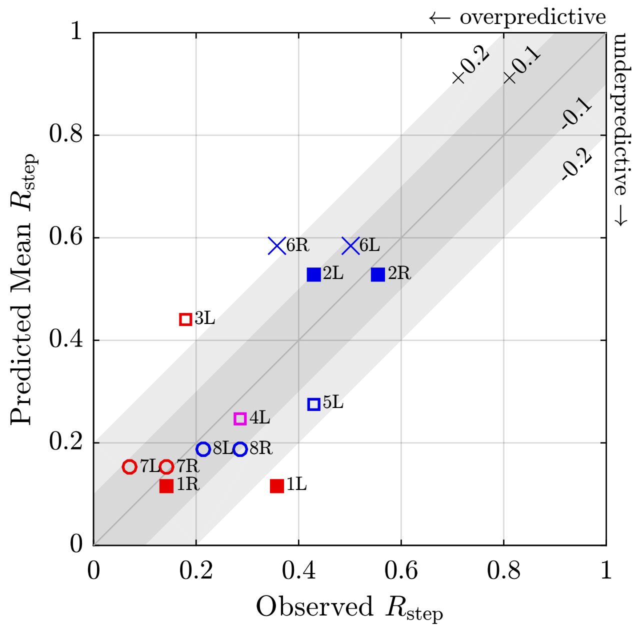

FIG. 13: Comparison of predicted and experimentally observed proportion of stepped failure along the fully fixed vertical edges of full-scale walls. Predicted values were calculated using mean values and CoVs of material properties measured experimentally. Data points are annotated by the wall id. number (1-8) and 'left' or 'right' edge.

However, due to uncertainty as to the extent of the perpend contribution, undertaking such an exercise is beyond the scope of this paper.

Tests on Full-Scale Walls

The accuracy of the proposed method for predicting the expected likelihood of the alternate failure modes was evaluated using out-of-plane cyclic loading tests on full-scale walls reported in Griffith et al. (2007). This data set included eight walls constructed using 230 × 110 × 76 mm cored clay brick units and 10 mm thick mortar joints. All walls were nominally 2.5 m tall (29 courses of bricks) and either 4.0 m (6×) or 2.5 m (2×) long; six of the eight walls had a window opening; and four of the walls were subjected to vertical precompression of either 0.05 or 0.10 MPa. Each wall had short return walls at its lateral edges which were restrained so as to create full moment fixity at the vertical edges of the main wall face (idealised support conditions depicted in Figure 2c). The walls were tested under cyclic face loading applied using airbags positioned on both faces of the wall. Upon loading, the walls underwent two-way bending which caused vertical cracks along the lateral edges. Further detail of these experimental arrangements is provided in Griffith et al. (2007).

The expected proportion of stepped failure was computed using equation (31). Material properties used as input in the analyses were quantified through tests on small-sized specimens using the same techniques as in the tests by Willis, described previously. The experimental value of R_{step} was determined by examining the crack patterns at the conclusion of the tests and counting the number of failed brick units and bed joints along the vertical edges of the walls. Note that in three of the walls, an asymmetrically positioned opening meant that the vertical crack was only partially developed along the edge closer to the opening, and these cases are ignored. A detailed summary of these analyses is presented in Table 2. Comparison of the predictions with experiment is shown in Figure 13. The method has favourable accuracy with the average error in R_{step} being equal to +0.01 (taken as the difference between the calculated and observed values). The precision of the predictions is also favourable, with nine of the 13 cases falling within the ± 0.1 band. The fact that these results show less scatter than results for the small-sized wallettes is consistent with an averaging effect due to a greater number of brick courses.

CONCLUDING REMARKS

This paper has described a pair of methodologies for the analysis of unreinforced brick masonry walls in horizontal bending which account for weak link effects involved in the crack formation process. The methods employ a probabilistic treatment of simplified design expressions for moment capacities of the stepped and line failure modes where the mechanical properties are represented as random variables.

The first method considers the ultimate bending strength of the mixed (combined stepped and line) failure mode, whose probability distribution functions are formulated by taking the strength as the lesser of the stepped and line failure modes. The strength reduction that occurs due to weak link effects was quantified for both the mean and characteristic values of ultimate strength, the latter being relevant toward design. These predictions indicate that for typical levels of material strength variability (CoV = 0.3) there can be up to a 17% reduction in strength compared to conventional design methodology; whilst at the upper end of variability levels observed in practice (CoV = 0.5) this reduction could be as high as 28%. It is emphasised that in its present state, the model described represents only a single 'element' comprising the two alternate failure modes (brick and bed joint) connected in series. Further work is planned to quantify expected strength reductions in full cracks consisting of multiple such elements connected in parallel, and to investigate the effect of load redistribution under different levels of element ductility. The resulting methodology has numerous possible applications: The moment capacity of the mixed failure mode may be directly incorporated into a generalised virtual work approach for estimating the ultimate out-of-plane strength of various types of out-of-plane failure mechanisms (Lawrence and Marshall 2000; Baker et al. 2005; Vaculik et al. 2014). The outcomes can furthermore be used to provide a rational basis for the development of a partial safety factor design procedure for ultimate out-of-plane strength design.

The purpose of the second method described in this paper is to estimate the expected likelihood of stepped failure versus line failure along vertical cracks. The proposed method shows good agreement with experimental tests on both small wallettes and full-sized walls. The usefulness of being able to predict the relative likelihood of the failure modes stems from their contrasting post-cracking behaviour—stepped cracks can maintain some residual frictional capacity, whereas line cracks are brittle and unable to carry any residual load (in typical non-arching wall configurations). Since previous experimental research (Willis et al. 2004) has demonstrated that the residual horizontal bending moment capacity of a vertical crack is effectively proportional to the amount of stepped failure along the crack, a direct implementation of the developed method is to use the predicted proportion of stepped failure [computed via equation (32)] as a strength reduction factor applied to the frictional post-cracking moment capacity (Vaculik et al. 2014). This residual moment capacity can then be implemented into a virtual work limit analysis approach for computing the overall residual strength of out-of-plane walls (i.e. in absence of any bond). A further potential application of the proposed method is the provide the basis for development of an analytical tool for checking whether vertical edge separation in two-way spanning walls is expected to occur following crack formation. The implication of these considerations is particularly important toward the out-of-plane seismic performance of wall panels.

ACKNOWLEDGEMENTS

This research was conducted with the financial support of the Australian Research Council (Grant No. DP0450933) and The University of Adelaide.

TABLE 1: Analytical and experimental results for wallettes tested by Willis et al. (2004).

Test Id.			Analysis inputs				Analysis results						Experimental		Comparison		
σ_v [MPa]	Dir.	Rep.	$\widehat{f}_{mt}$ [MPa]	$\mathbb{C}\langle f_{mt}\rangle$	F_{ut}	Σ_v	η_{step}	η_{line}	η_{min}	η_{mix}	ϕ_{mean}	R_{step}	η	R_{step}	$\eta_{\text{min}}/\eta_{\text{test}}$	$\eta_{\text{mix}}/\eta_{\text{test}}$	$(R_{\text{step}})_{\text{calc}}-(R_{\text{step}})_{\text{test}}$
0	H	1	0.78	0.14	6.41	0	3.25	2.78	2.78	2.62	0.94	0.29	2.88	0.6	0.96	0.91	−0.31
		2	0.78	0.14	6.41	0	3.25	2.78	2.78	2.62	0.94	0.29	2.47	0.6	1.13	1.06	−0.31
		3	0.74	0.23	6.76	0	3.25	2.93	2.93	2.65	0.90	0.38	3.31	0.6	0.89	0.80	−0.22
		4	0.74	0.23	6.76	0	3.25	2.93	2.93	2.65	0.90	0.38	3.16	0.2	0.93	0.84	+0.18
		5	0.58	0.31	8.62	0	3.25	3.74	3.25	2.91	0.90	0.64	4.87	0.6	0.67	0.60	+0.04
0	V	1	0.67	0.24	7.46	0	3.25	3.23	3.23	2.79	0.86	0.50	2.99	1.0	1.08	0.93	−0.50
		2	0.67	0.24	7.46	0	3.25	3.23	3.23	2.79	0.86	0.50	3.36	1.0	0.96	0.83	−0.50
		3	0.67	0.24	7.46	0	3.25	3.23	3.23	2.79	0.86	0.50	3.32	1.0	0.98	0.84	−0.50
		4	0.67	0.24	7.46	0	3.25	3.23	3.23	2.79	0.86	0.50	3.88	1.0	0.83	0.72	−0.50
		5	0.56	0.10	8.93	0	3.25	3.87	3.25	3.09	0.95	0.72	3.39	1.0	0.96	0.91	−0.28
0.075	V	1	0.78	0.14	6.41	0.10	3.42	2.77	2.77	2.65	0.96	0.22	3.90	0.2	0.71	0.68	+0.02
		2	0.78	0.14	6.41	0.10	3.42	2.77	2.77	2.65	0.96	0.22	3.62	0.6	0.76	0.73	−0.38
		3	0.56	0.10	8.93	0.13	3.49	3.86	3.49	3.25	0.93	0.64	4.22	1.0	0.83	0.77	−0.36
		4	0.58	0.31	8.62	0.13	3.48	3.73	3.48	3.05	0.88	0.57	4.58	1.0	0.76	0.67	−0.43
		5	0.58	0.31	8.62	0.13	3.48	3.73	3.48	3.05	0.88	0.57	3.96	1.0	0.88	0.77	−0.43
0.15	V	1	0.68	0.26	7.35	0.22	3.65	3.17	3.17	2.91	0.92	0.34	3.51	0.6	0.90	0.83	−0.26
		2	0.68	0.26	7.35	0.22	3.65	3.17	3.17	2.91	0.92	0.34	3.39	0.4	0.93	0.86	−0.06
		3	0.68	0.26	7.35	0.22	3.65	3.17	3.17	2.91	0.92	0.34	3.17	0.6	1.00	0.92	−0.26
		4	0.56	0.10	8.93	0.27	3.74	3.85	3.74	3.38	0.90	0.54	4.51	0.6	0.83	0.75	−0.06
		5	0.68	0.26	7.35	0.22	3.65	3.17	3.17	2.91	0.92	0.34	3.89	1.0	0.81	0.75	−0.66
0.25	V	1	0.59	0.20	8.48	0.42	4.02	3.64	3.64	3.34	0.92	0.37	5.19	0.6	0.70	0.64	−0.23
		2	0.59	0.20	8.48	0.42	4.02	3.64	3.64	3.34	0.92	0.37	5.13	0.4	0.71	0.65	−0.03
		3	0.59	0.20	8.48	0.42	4.02	3.64	3.64	3.34	0.92	0.37	4.83	0.2	0.75	0.69	+0.17
		4	0.59	0.20	8.48	0.42	4.02	3.64	3.64	3.34	0.92	0.37	3.99	0.6	0.91	0.84	−0.23
		5	0.56	0.10	8.93	0.45	4.06	3.83	3.83	3.51	0.92	0.41	3.37	0.6	1.14	1.04	−0.19
														Mean:	0.88	0.80	−0.25
														St. Dev:	0.13	0.12	0.22
														CoV:	0.15	0.15	

Notes:
· Clay brick units had nominal dimensions 230 × 114 × 65 mm and 10 mm mortar joints.
· Brick modulus of rupture mean and CoV: $\widehat{f}_{ut} = 5.00$ MPa, $\mathbb{C}\langle f_{ut}\rangle = 0.26$.
· Self-weight of specimens was considered negligible relative to the applied axial stress.
· 'Dir' denotes specimen orientation during test. 'H' = tested horizontally, 'V' = tested vertically.
· η_{min} denotes the direct minimum of the predicted values for stepped and line failure; i.e. $\eta_{\text{min}} = \min(\eta_{\text{step}}, \eta_{\text{line}})$.
· Strength reduction factor for mean strength was taken as $\phi_{\text{mean}} = \eta_{\text{mix}}/\eta_{\text{min}}$.
· Observed R_{step} was taken as $n_b/5$, where n_b was the number of failed bed joints over a total of 5 bed joints that could potentially fail.

TABLE 2: Predicted and observed proportion of stepped failure along the vertical edge cracks in full-scale test panels tested by Griffith et al. (2007).

Wall	Analysis inputs and results						Experimental results								Error in R_{step}	
	$\widehat{f}_{mt}$	$\mathbb{C}\langle f_{mt}\rangle$	σ_v	F_{ut}	Σ_v	R_{step}	Left edge				Right edge				(calc − test)	
	[MPa]		[MPa]				n_b	n_u	uncr	R_{step}	n_b	n_u	uncr	R_{step}	L edge	R edge
S1	0.721	0.199	0.124	4.92	0.172	0.12	10	9	0	0.36	4	12	0	0.14	−0.24	−0.03
S2	0.520	0.266	0.024	6.83	0.046	0.53	12	8	0	0.43	15	6	1	0.56	+0.10	−0.03
S3	0.499	0.280	0.135	7.11	0.270	0.44	5	11.5	0	0.18	–	–	–	–	+0.26	–
S4	0.639	0.212	0.079	5.56	0.124	0.25	8	10	0	0.29	–	–	–	–	−0.04	–
S5	0.655	0.212	0.024	5.42	0.037	0.28	12	8	0	0.43	–	–	–	–	−0.15	–
S6	0.496	0.217	0.024	7.16	0.048	0.58	14	7	0	0.50	10	9	0	0.36	+0.08	+0.23
S7	0.682	0.226	0.145	5.21	0.212	0.15	2	13	0	0.07	4	12	0	0.14	+0.08	+0.01
S8	0.714	0.194	0.025	4.97	0.034	0.19	6	11	0	0.21	8	10	0	0.29	−0.03	−0.10
														Mean:	+0.01	
														St. Dev:	0.14	

Notes:
· Brick modulus of rupture mean and CoV: $\widehat{f}_{ut} = 3.55$ MPa, $\mathbb{C}\langle f_{ut}\rangle = 0.267$.
· Vertical compressive stress (σ_v) used to calculate Σ_v was taken as the average value at the mid-height of the wall.
· n_u = number of units undergoing line failure; n_b = number of bed joints undergoing stepped failure.
· 'uncr' denotes number of courses remaining uncracked (undergoing neither stepped nor line failure).
· Each panel had a total of 29 courses; hence, the observed proportion of stepped failure was taken as $R_{\text{step}} = n_b/(29-1)$.

REFERENCES

Baker, C., Chen, B., and Drysdale, R. (2005). "Failure line method applied to walls with openings." *10th Canadian Masonry Symposium*, Banff, Alberta, Canada.

Baker, L. R. and Franken, G. L. (1976). "Variability aspects of the flexural strength of brickwork." *4th International Brick Masonry Conference*, Brussels.

Base, G. D. and Baker, L. R. (1973). "Fundamental properties of structural brickwork." *Journal of the Australian Ceramic Society*, 9(1), 1–6.

Casapulla, C. and Portioli, F. (2015). "Experimental and analytical investigation on the frictional contact behavior of 3D masonry block assemblages." *Construction and Building Materials*, 78, 126–143.

Comité Européen de Normalisation (2005). *Eurocode 6, Design of Masonry Structures—Part 1-1: General rules for reinforced and unreinforced masonry structures.* CEN, Brussels, Belgium, EN 1996-1-1:2005 (E) edition.

Foraboschi, P. (2014). "Resisting system and failure modes of masonry domes." *Engineering Failure Analysis*, 44, 315–337.

Foraboschi, P. and Vanin, A. (2013). "Non-linear static analysis of masonry buildings based on a strut-and-tie modeling." *Soil Dynamics and Earthquake Engineering*, 55, 44–58.

Griffith, M. C. and Vaculik, J. (2007). "Out-of-plane flexural strength of unreinforced clay brick masonry walls." *TMS Journal*, 25(1), 53–68.

Griffith, M. C., Vaculik, J., Lam, N. T. K., Wilson, J., and Lumantarna, E. (2007). "Cyclic testing of unreinforced masonry walls in two-way bending." *Earthquake Engineering and Structural Dynamics*, 36(6), 801–821.

Heffler, L. M., Stewart, M. G., Masia, M. J., and Correa, M. R. S. (2008). "Statistical analysis and spatial correlation of flexural bond strength for masonry walls." *Masonry International*, 21(2), 59–70.

Lagomarsino, S. (2015). "Seismic assessment of rocking masonry structures." *Bulletin of Earthquake Engineering*, 13(1), 97–128.

Lawrence, S. (1991). "Stochastic analysis of masonry structures." *International Symposium on Computer Methods in Structural Masonry*, Swansea, United Kingdom, 104–113.

Lawrence, S. and Marshall, R. (2000). "Virtual work design method for masonry panels under lateral load." *12th International Brick and Block Masonry Conference*, Vol. 2, Madrid, Spain, 1063–1072.

Lawrence, S. J. (1985). "Random variations in brickwork properties." *7th International Brick Masonry Conference*, Melbourne, Australia, 537–547.

Lawrence, S. J. (1995). "The behaviour of masonry in horizontal flexure." *7th Canadian Masonry Symposium*, Hamilton, Ontario, 525–536.

Lawrence, S. J. and Cao, H. T. (1988). "Cracking of non-loadbearing masonry walls under lateral forces." *8th International Brick and Block Masonry Conference*, Dublin, 1184–94.

Lawrence, S. J. and Lu, J. P. (1991). "An elastic analysis of laterally loaded masonry walls with openings." *International Symposium on Computer Methods in Structural Masonry*, Swansea, United Kingdom, 39–48.

Li, J., Masia, M. J., and Stewart, M. G. (2016a). "Stochastic spatial modelling of material properties and structural strength of unreinforced masonry in two-way bending." *Structure and Infrastructure Engineering*, In Press, 1–13.

Li, J., Masia, M. J., Stewart, M. G., and Lawrence, S. J. (2014). "Spatial variability and stochastic strength prediction of unreinforced masonry walls in vertical bending." *Engineering Structures*, 59, 787–797.

Li, J., Stewart, M. G., Masia, M. J., and Lawrence, S. J. (2016b). "Spatial correlation of material properties and structural strength of masonry in horizontal bending." *Journal of Structural Engineering*, 142(11).

Lu, J. P. and Lawrence, S. J. (1991). "Cracking of laterally loaded masonry walls with openings." *9th International Brick and Block Masonry Conference*, Berlin, Germany, 1087–94.

McNeilly, T., Scrivener, J., Lawrence, S., and Zsembery, S. (1996). "A site survey of masonry bond strength." *Australian Civil/Structural Engineering Transactions*, CE38(2, 3 & 4), 103–109.

Orduña, A. and Lourenço, P. B. (2005). "Three-dimensional limit analysis of rigid blocks assemblages. Part II: Load-path following solution procedure and validation." *International Journal of Solids and Structures*, 42(18-19), 5161–5180.

Schueremans, L. and Gemert, D. V. (2006). "Probability density functions for masonry material parameters—A way to go?." *5th International Conference on Structural Analysis of Historical Constructions*, New Delhi, India.

Seward, D. W. (1982). "A developed elastic analysis of lightly loaded brickwork walls with lateral loading." *International Journal of Masonry Construction*, 2(3), 129–123.

Sinha, B. P. (1978). "A simplified ultimate load analysis of laterally loaded model orthotropic brickwork panels of low tensile strength." *The Structural Engineer*, 56B(4), 81–84.

Standards Australia (2011). *Australian Standard for Masonry Structures (AS 3700—2011)*. SA, Sydney, NSW.

Stewart, M. G. and Lawrence, S. J. (2002). "Structural reliability of masonry walls in flexure." *Masonry International*, 15(2), 48–52.

Timoshenko, S. P. and Goodier, J. N. (1934). *Theory of Elasticity*. McGraw-Hill Book Company, New York, third (1970) edition.

Vaculik, J. (2012). "Unreinforced masonry walls subjected to out-of-plane seismic actions." PhD thesis, The University of Adelaide, South Australia.

Vaculik, J., Griffith, M. C., and Magenes, G. (2014). "Dry stone masonry walls in bending—Part II: Analysis." *International Journal of Architectural Heritage*, 8(1), 29–48.

Willis, C. R. (2004). "Design of unreinforced masonry walls for out-of-plane loading." PhD thesis, University of Adelaide, South Australia.

Willis, C. R., Griffith, M. C., and Lawrence, S. J. (2004). "Horizontal bending of unreinforced clay brick masonry." *Masonry International*, 17(3), 109–121.

APPENDIX I. NOTATION

The following symbols are used in this paper.

Variables and Operators:

$\mathbb{C}\langle X \rangle$ = coefficient of variation of X;
$\mathrm{Char}\langle X \rangle$ = characteristic value of X;
$\mathbb{E}\langle X \rangle$ = mean value of X;
f_{mt} = flexural tensile strength of the bond;
f_{ut} = tensile modulus of rupture of the brick unit;
F_{ut} = ratio of mean f_{ut} to mean f_{mt};
G_h = geometric constant;
h_u = height of brick unit;
k_{be} = elastic torsion constant for rectangular section;
k_{line} = geometric constant for line failure;
k_{step} = geometric constant for stepped failure;
l_u = length of brick unit;
m_u = ultimate moment per course of the masonry;
$\bar{M}$ = moment per unit length of the crack;
n = total number of courses;
$p_X(x)$ = PDF of variable X at value x;
P_{line} = probability of line failure;
P_{step} = probability of stepped failure;
$P_X(x)$ = CDF of variable X at value x;
r = bond shear strength coefficient for f_{mt};
R_{step} = proportion of stepped failure along a crack;

s_b = bed joint overlap;
$\mathbb{S}\langle X \rangle$ = standard deviation of X;
t_j = thickness of mortar joint;
t_u = thickness of brick unit;
$\widehat{X}$ = mean value of X;
η = orthogonal strength ratio;
μ = bond shear strength coefficient for σ_v;
ν_u = Poisson's ratio of brick unit;
σ_v = vertical axial stress;
Σ_v = ratio of σ_v to mean f_{mt};
τ_{um} = ultimate shear capacity of the bond; and
ϕ = strength reduction factor.

Subscripts:

char = characteristic strength;
const = constant component;
line = line failure;
mean = mean strength;
mix = mixed failure (stepped and line);
rand = random component; and
step = stepped failure.